Unified path for high-pressure transitions of SiC polytypes to the rocksalt structure

M. S. Miao and Walter R. L. Lambrecht
Department of Physics, Case Western Reserve University, Cleveland, Ohio 44106-7079, USA
(Received 18 June 2003; published 9 September 2003)

A common strain induced transition path is proposed for the high pressure transformation of the various tetrahedrally bonded polytypes of SiC to the rocksalt structure. The energy barriers associated with these transition paths are calculated using a first principles pseudopotential method, including suitably constrained relaxations. The 3C transition is found to have a lower enthalpy barrier than the other polytypes at pressures above the equilibrium transition pressure.

DOI: 10.1103/PhysRevB.68.092103 PACS number(s): 61.50.Ks, 81.30.Hd

The transition from the (mostly) covalent fourfold coordinated structures, such as zinc blende (ZB) or wurtzite (WZ), to the (mostly) ionic sixfold coordinated rocksalt (RS) structure for semiconductors has been intensively studied both theoretically and experimentally.[1,2] Recent work has focused on transition paths between these structures and their enthalpy barriers.[3–10] These transition paths are concerned with the collective motion of the atoms relevant to the nucleation stage of the phase transition and not with the subsequent adaptation of the transformed phase inside the host, which is mediated by dislocations. The transition paths proposed so far are rather different for ZB→RS (Refs. 6–10) and for WZ→RS.[4,5] Here, we point out that these transition paths can be described as special cases of a general path valid for all tetrahedrally bonded polytypes. As is well known, SiC exhibits polytypism, i.e., a large number of different crystal structures differing from each other only in the periodic stacking sequence of the same hexagonal bilayers as the hexagonal (0001) or cubic (111) planes. In the ZB (or 3C) case, the proposed path is a new, monoclinic, path, which is, however, closely related to the previously proposed orthorhombic path, while in the WZ (or 2H) case it is exactly the same orthorhombic path as proposed before. While it has recently been pointed out that the previous paths correspond to high symmetry paths which could be found by group theoretical arguments,[11] the occurence of a lower barrier monoclinic path shows that the underlying assumption of a maximally high symmetry along the path can be misleading.

Although first-principles calculations[12,13] predict phase transitions to occur at similar pressures for the various common polytypes of SiC (4H, 6H, and 3C), namely, at about 65 ± 5 GPa, only the transition from 3C to RS has been observed in static diamond-anvil cell (DAC) experiments and at a much higher pressure of about 100 GPa,[14] although 6H was also investigated. The transition from 6H has only recently been observed in shock compression experiments[15] at a pressure of 105 GPa.

The common transition path envisioned here is illustrated in Fig. 1. The stackings of 2H, 4H, 6H, and 3C, indicated by the full zigzag lines, correspond to a periodic repeat of the *AB*, *ABCB*, *ABCACB*, *ABC* repeat units, respectively, where *A*, *B*, and *C* indicate the position of, e.g., the Si atoms in the hexagonal layer. The transition to the RS structure involves four structural distortions. First, there is a uniaxial traceless compression along the hexagonal $[10\bar{1}0]$ direction, which we will call the γ shear. It changes the angle between the basis vectors in the basal plane from 60° (hexagonal) to 90° (square), as shown in the top inset of Fig. 1. Second, there is a relative shift of the layers, which in the case of 3C is also a shear, but in other cases, corresponds to an internal degree of freedom of the unit cell. We will call this the β or ''layer shuffle'' move. The shifted positions are indicated by the dashed lines in Fig. 1. If we measure lateral positions in units of the $[10\bar{1}0]A$ to *A* distance the original *B* and *C* positions are at 1/3 and 2/3, whereas the new positions correspond either to integer or half integer values. These changes can be denoted as $ABCABC\cdots$ to $0\frac{1}{2}1\frac{3}{2}2\frac{5}{2}3\cdots$ for 3C. Correspondingly, for 2H, the changes are from $ABABAB\cdots$ to $0\frac{1}{2}0\frac{1}{2}0\frac{1}{2}0\cdots$, and for 4H, $ABCBABCB\cdots$ to $0\frac{1}{2}1\frac{1}{2}0\frac{1}{2}1\frac{1}{2}0\cdots$. For 3C, the net result of the above two movements is that the two edge-attached tetrahedra change to an (irregular) octahedron (see bottom inset of Fig. 1). Note that here we consider both filled and empty nearest neighbor Si-Si tetrahedra. For 2H, the octahe-

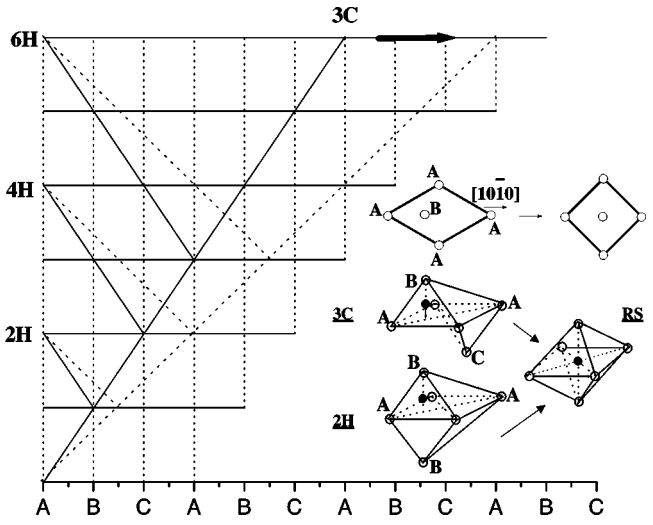

FIG. 1. Stacking sequence in hexagonal and cubic polytypes and their transformation through a layer shuffle movement to rocksalt. The top inset show the in-plane γ shear. The bottom inset shows how adjacent tetrahedra join into an octahedron for 3C and 2H. Open (closed) spheres are Si (C).

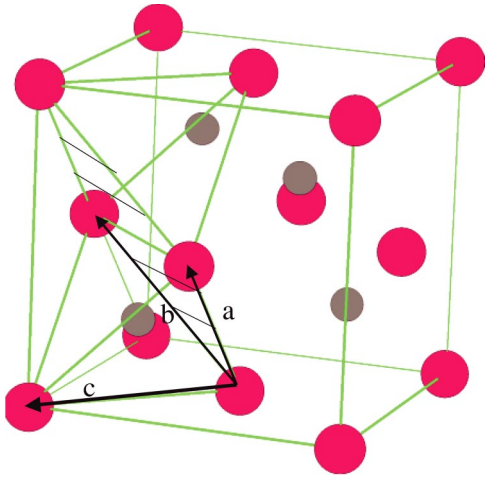

FIG. 2. Relation between the monoclinic intermediate state unit cell and the conventional cubic unit cell of 3C. See text.

dron results from two face-attached tetrahedra right on top of each other and two adjacent empty distorted tetrahedra, as is also illustrated in the bottom inset. A mixture of these two kinds of local structural changes occurs for the other polytypes. The above two collective motions define basically the rearrangement of the tetrahedral structure to an octahedral one. Accompanying these distortions, the interlayer distances are reduced and, finally, a relative movement occurs between the C and Si sublattices. As shown in the inset of Fig. 1, C moves from its original position 1/4 above the basal plane to the basal plane and so fills the center of the newly formed octahedral site. We emphasize that all of the above motions do not occur sequentially but simultaneously. Overall, the strains combine to a considerable volume compression because during the transition two new bonds are formed while none are broken.

This path is the same as the previously proposed orthorhombic path for WZ (Ref. 4) and a logical generalization of it for other hexagonal polytypes such as 4H and 6H. Figure 2 reveals the relation to the previously proposed orthorhombic path for the 3C transition.[6] The vectors $(\vec{a},\vec{b},\vec{c})$ construct the primitive cell for the intermediate state. During the transition, the cell changes from the ZB geometry $(a=b=c,\alpha=\beta=\gamma=60°)$ to the RS geometry $(a=b=c,\alpha=\beta=60°,\gamma=90°)$ through a series of intermediate states with monoclinic symmetry $(a=b\neq c,\alpha=\beta\neq\gamma)$. If a supplementary condition, $(\vec{a}+\vec{b}-\vec{c})\cdot\vec{c}=0$ is satisfied, there is orthorombic symmetry, and the lattice vectors of an orthorhombic cell (cell III in Ref. 6) are $a_c=\vec{a}-\vec{b}, b_c=\vec{c}$, and $c_c=\vec{a}+\vec{b}-\vec{c}$.

As discussed extensively in two previous papers,[8,9] a description similar to the above does not yet completely describe the transition path because of the multidimensionality of the parameter space. To fully specify a path, we need to identify one of the collective motions as the ''reaction coordinate'' and show that the other motions are induced by it using total enthalpy minimization. Since the relative displacements of the C relative to the Si sublattice correspond to high-frequency optical phonon modes, they should clearly follow the strain rather than causing it. Among the strains, we need to pick the symmetry breaking γ shear mode. Thus, we adopt the γ shear mode as reaction coordinate and perform a complete relaxation of all other degrees of freedom. Although imposing a shear strain implies that the stress is no longer hydrostatic throughout the sample, we view this as the long-wavelength limit of a near zone center acoustical phonon fluctuation.

We perform plane wave pseudopotential calculations for 2H, 3C, 4H, and 6H at pressures of 0, 30, 63, 93, and 120 GPa. The Troullier-Martins pseudopotentials[16] are used with core radii of 1.3 Å for C and 2.5 Å for Si. The energy cutoff was tested and set at 60 Ry. The Perdew-Wang generalized gradient approximated[17] (GGA) exchange-correlation energy functional and potential is adopted. The geometry optimization is done using a modified variable-cell-shape[18] (VCS) dynamics which changes the positions of the ions and the components of the metric **g** (the dot products between the lattice vectors of the simulation cell). During the calculation we constrain $g_{12}/g_{11}=(\vec{a}\cdot\vec{b})/(\vec{a}\cdot\vec{a})=\zeta$ which is equivalent to keeping the angle γ fixed to a given value. The other metric elements and atom positions are fully relaxed. In another set of calculations for 3C, we further constrain $g_{33}=g_{13}+g_{23}$, i.e., $\vec{c}\cdot\vec{c}=\vec{a}\cdot\vec{c}+\vec{b}\cdot\vec{c}$, which enforces the orthorhombic symmetry.

The calculated lattice parameters and bulk moduli for the different polytypes are to within 1 and 5 % of previous calculations.[13] The equilibrium transition pressures are found to be 63, 60, 58, and 58 GPa for 3C, 2H, 4H, and 6H. This differs from previous predictions,[13] which found a slightly higher transition pressure for 4H and 6H than for 3C. The corresponding transition volumes V_t/V_0, with V_0 the equilibrium volume, are about 0.80 ± 0.02 and the volume change ΔV at the transition pressure is about 18 % for all polytypes, and remains nearly constant at higher pressures. The calculated ΔV is in good agreement with the experimental value of 20.3 % for 3C.

Figure 3 shows the enthalpy barriers for 2H, 3C, 4H, and 6H polytypes as a function of pressure. The enthalpy barrier decreases quickly with increasing pressure. Above the transition pressure, 3C shows a distinctly lower enthalpy barrier than the other polytypes. This might be related to the fact that in the 3C case, the layer shuffle corresponds to a uniform shear, whereas in the other polytypes, it corresponds to an internal structural parameter. This distinct behavior of 3C may also provide an explanation for why experimentally it has apparently been more difficult to observe the transition to RS for polytypes other than 3C. Our calculations do not support a higher transition pressure for noncubic polytypes but do support a higher enthalpy barrier. It would be useful in future experimental work to search for differences in the hysteresis cycle between 3C and hexagonal polytypes.

Next, we examine the 3C results in some more detail to confirm that the present monoclinic path has indeed a lower enthalpy barrier than the closely related orthorhombic path. This is illustrated in Fig. 4 for both 0 and 63 GPa. The inset shows the deviation from the ideal orthorhombic structure at 120 GPa. The maximum deviations happen near but not exactly at the transition state. This deviation becomes stronger

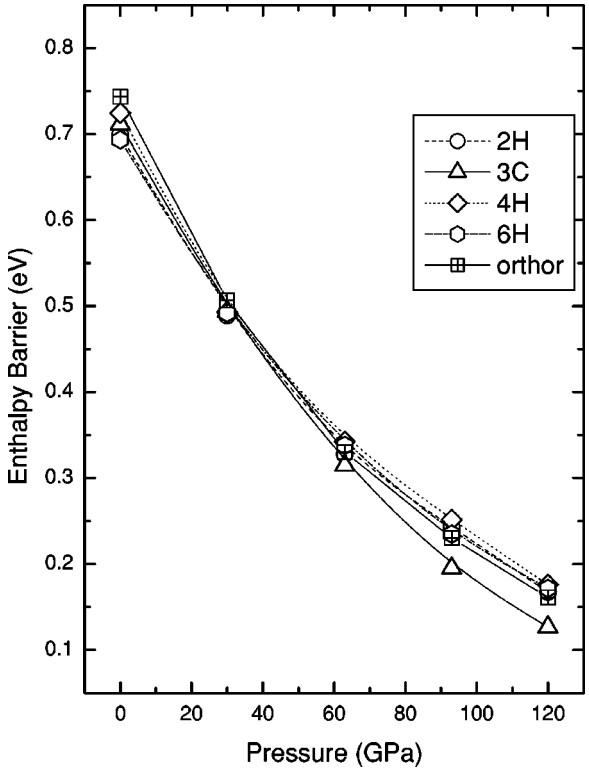

FIG. 3. Enthalpy barriers of the transitions to RS for the SiC polytypes as function of pressure.

at higher pressure. We also point out here that the MD simulation of Shimojo *et al.*[10] missed this small deviation from orthorhombic symmetry. Although these VCS-MD simulations allow for arbitrarily low symmetry in principle, they nevertheless appear to have some tendency towards higher symmetry structures. In fact, a close inspection of Fig. 3 of Ref. 10 shows that in the time region 3.3 ps$\leqslant t$ $\leqslant$3.45 ps, $L_1=L_2\neq L_3$, but $\alpha=\beta=\gamma=90°$, meaning that their system goes from cubic to orthorhombic via an intermediate tetragonal structure. This occurs even though there is no apparent reason for it according to the calculations of the energy landscape.[9]

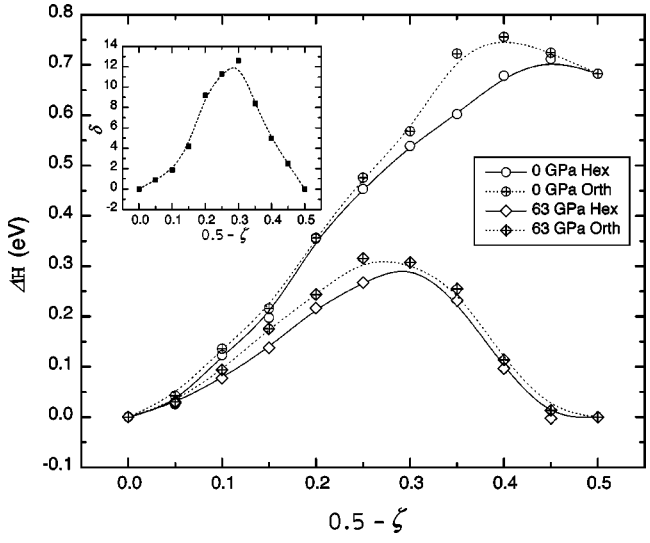

FIG. 4. Enthalpy changes along the orthorhombic and the monoclinic paths to rocksalt at 0 and 63 GPa. The inset shows the deviation from the ideal orthorhombic structure, in which $\delta=(g_{13}+g_{23}-g_{33})/g_{33}$ (in %). For the orthorhombic structure, $\delta=0$.

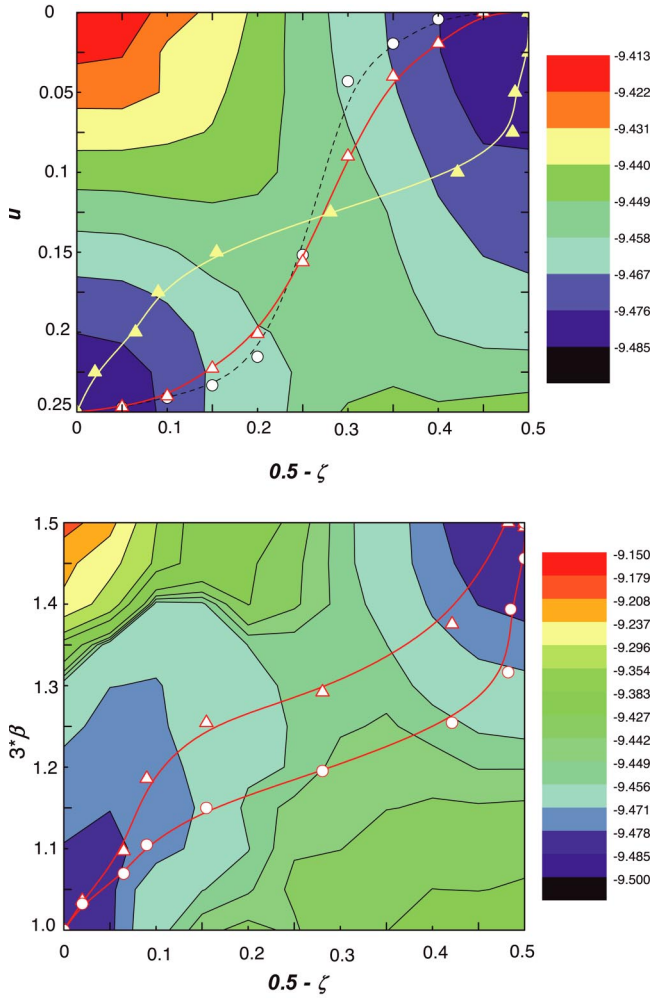

FIG. 5. (Color online) Contour plot of enthalpy (in Ry/pair) of 3C as function of (a) shear strain $\gamma=0.5-\zeta$, and sublattice coordinate u, (b) shear strains γ and $\beta=g_{13}/g_{11}$. The enthalpy is minimized against all the other parameters. The left hand lower corner corresponds to ZB, the upper right hand corner corresponds to RS. The FSP (fixed γ strain path) (open triangles) and FPP (fixed u position path) (filled triangles) for 3C and the FSP for 2H (open circles) are also shown in (a) and the FSP for both 3C (triangles) and 2H (circles) are shown in (b).

It is of interest to further study the interdependence of the various collective atomic motions participating in the path. Figure 5 shows two hypersurfaces of the enthalpy in the multidimensional parameter space for 3C-SiC. Here two variables are varied independently and the remaining ones are relaxed. Superposed on this are shown specific paths, along which one of the variables is kept fixed and the other relaxed. These show a distinct nonlinear behavior, which was discussed in more detail in Ref. 9 for the orthorhombic path. Along the FSP (fixed strain path) one can see that initially the u value barely changes. It is only beyond a certain thresh-

old of γ that u suddenly starts to change quickly. Likewise, once it approaches the RS strain, u quickly jumps to the value for RS. Similarly, if we were to fix the positions first, which admittedly is somewhat unphysical, the strain has initially a tendency to stay close to its starting value. In both cases, we might call this an ''initially delayed'' response. The crossing point of the two curves corresponds approximately (and very closely) to the transition state (TS) where the barrier is maximum. Our barrier is a slight upper limit because there is a second internal parameter, the optimal value of which may not be exactly the same along the two curves.

The paths in $\gamma-\beta$ space behave differently. Here, the delay of the response occurs in the intermediate value range of the reaction coordinate, while the fast behavior occurs near the endpoints. This shows that the layer shuffle is strongly coupled to the γ strain in the ZB and in the RS state but not in the intermediate state. It is worth noticing that this delay is more prominent for 2H, indicating that the interlayer shifts are harder for 2H. This observation is consistent with the fact that hexagonal polytypes have higher barrier than 3C at a pressure higher than the transition pressure. In Fig. 5(a), the 2H FSP path also shows a larger delay than the 3C FSP path, indicating that sublattice movements respond slower than those in 3C to γ strain. This may be caused by the slow response of the β strain for 2H.

The strains considered here can be considered as the long-wavelength limit of certain acoustic phonons. The phonons corresponding to the strains γ and β have a propagation direction along [112] and [111], respectively, both with a polarization in the [110] direction. The sound velocities for these cases were studied in Ref. 19 as function of pressure and were found to have negative mode Grüneisen parameters $d\ln\omega/d\ln V$ when calculated at the transition pressure. This indicates a softening (although not to the point of an elastic instability) of the corresponding phonons at the zone center under high pressure. In contrast to the acoustic phonons, all the optic phonons are hardened by increasing pressure.[20–22] While phonon mode softening has been considered before in the context of these phase transitions by Weinstein,[2] he considered zone-boundary phonons, whereas in our present discussion the zone-center ones are identified to be the relevant ones.

Our view of the transition mechanism can be summarized as follows. At the equilibrium transition pressure, defined by the common tangent of the two equations of state, the enthalpy barrier between the two phases is too high for the transition to be allowed kinetically. However, with further increasing pressure, the zone center acoustic phonons corresponding to the γ strain become gradually softer. The layer shuffle (which corresponds to a monoclinic β strain in the 3C case) and the intersublattice motion (corresponding to optical phonons) are stronlgy coupled to the γ strain and follow it. In fact, the shuffle motion also become softer with increasing pressure. Beyond a certain value of the γ strain, there is a transition where the optic modes (sublattice displacements) become unstable because now some atoms become within reach to form new bonds. One of these is in the basal plane, and the second results from the interlayer distance reduction. This locks the structure in a more symmetric position accompanied by a contraction of the layers and a collapse of the volume.

In conclusion, a unified description for the nucleation stage of the phase transition from any tetrahedrally bonded polytype to RS was presented. The proposed mechanism involves several strains and intersublattice motions, whose interdependence was studied by means of first-principles enthalpy calculations. Slight, but possibly meaningful differences between 3C and the hexagonal polytypes were pointed out.

This work was supported by the Office of Naval Research.

[1] J. R. Chelikowsky and J. K. Burdett, Phys. Rev. Lett. **56**, 961 (1986).
[2] B. A. Weinstein, Solid State Commun. **24**, 595 (1977).
[3] M. A. Blanco, J. M. Recio, A. Costales, and R. Pandey, Phys. Rev. B **62**, 10 599 (2000).
[4] S. Limpijumnong, and W. R. L. Lambrecht, Phys. Rev. Lett. **86**, 91 (2001).
[5] S. Limpijumnong and W. R. L. Lambrecht, Phys. Rev. B **63**, 104103 (2001).
[6] M. Catti, Phys. Rev. Lett. **87**, 035504 (2001).
[7] M. Catti, Phys. Rev. B **65**, 224115 (2002).
[8] M. S. Miao, M. Prikhodko, and W. R. L. Lambrecht, Phys. Rev. Lett. **88**, 189601 (2002).
[9] M. S. Miao, M. Prikhodko, and W. R. L. Lambrecht, Phys. Rev. B **66**, 064107 (2002).
[10] F. Shimojo, I. Ebbsjö, R. K. Kalia, A. Nakano, J. P. Rino, and P. Vashishta, Phys. Rev. Lett. **84**, 3338 (2000).
[11] J. M. Perez-Mato, M. Aroyo, C. Capillas, P. Blaha, and K. Schwarz, Phys. Rev. Lett. **90**, 049603 (2003).
[12] K. J. Chang and M. L. Cohen, Phys. Rev. B **35**, 8196 (1987).
[13] K. Karch, F. Bechstedt, P. Pavone, and D. Strauch, Phys. Rev. B **53**, 13 400 (1996).
[14] M. Yoshida, A. Onodera, M. Ueno, K. Takemura, and O. Shimomura, Phys. Rev. B **48**, 10 587 (1993).
[15] T. Sekine and T. Kobayashi, Phys. Rev. B **55**, 8034 (1997).
[16] N. Troullier and J. L. Martins, Phys. Rev. B **43**, 1993 (1991).
[17] J. P. Perdew and Y. Wang, Phys. Rev. B **45**, 13 244 (1992).
[18] I. Souza and J. L. Martins, Phys. Rev. B **55**, 8733 (1997).
[19] M. Prikhodko, M. S. Miao, and Walter R. L. Lambrecht, Phys. Rev. B **66**, 125201 (2002).
[20] B. H. Cheong, K. J. Chang, and M. L. Cohen, Phys. Rev. B **44**, 1053 (1991).
[21] C. Wang, R. Yu, and H. Krakauer, Phys. Rev. B **53**, 5430 (1996).
[22] G. Wellenhofer, K. Karch, P. Pavone, U. Rössler, and D. Strauch, Phys. Rev. B **53**, 6071 (1996).